Environ. Sci. Technol. **2009,** *43,* 3542–3548

Weathering and the Fallout Plume of Heavy Oil from Strong Petroleum Seeps Near Coal Oil Point, CA

CHRISTOPHER FARWELL,[†] CHRISTOPHER M. REDDY,[‡] EMILY PEACOCK,[‡] ROBERT K. NELSON,[‡] LIBE WASHBURN,[§] AND DAVID L. VALENTINE*,[†]

Department of Earth Science and Marine Science Institute, University of California, Santa Barbara, California 93106, Department of Marine Chemistry and Geochemistry, Woods Hole Oceanographic Institution, Woods Hole, Massachusetts 02543, and Department of Geography and Marine Science Institute, University of California, Santa Barbara, California 93106

Received September 11, 2008. Revised manuscript received December 28, 2008. Accepted January 6, 2009.

Ⓦ This paper contains enhanced objects available on the Internet at http://pubs.acs.org/est.

The Coal Oil Point (COP) seeps offshore Goleta, CA, are estimated to release 20−25 tons of oil daily, providing an ideal natural laboratory to investigate the fate of oil in the coastal ocean. To address the long-term fate of COP oil, we collected 15 sediment samples down current from the seeps and quantified petroleum content and individual biomarkers using traditional and comprehensive two-dimensional gas chromatography. Similarities in the distributions of hopane biomarkers link the oil in the sediments to fresh seep oil ($n = 5$) and underlying reservoirs ($n = 3$), although sediment oil is heavily weathered. The spatial distribution of oil forms a plume along the continental shelf that we suggest represents a chronic fallout pattern for heavy oil from the persistent surface slicks; average surface currents appear to modulate the distribution of the fallout over a period of 0.4−5 days. The extent of hydrocarbon loss is consistent for all sediments, indicating a common limit to oil weathering with contributions from evaporation, biodegradation, and dissolution. Considering the amount of oil and quantity of sediment impacted, we estimate a sediment oil burden of 0.3×10^{12} to 3×10^{12} g in the study area, equivalent to 8−80 spills of the *Exxon Valdez* accident of 1989.

Introduction

A decreasing global supply of light crude oil is leading to increases in production, transportation, and use of heavier oils (*1*). One concern stemming from increased offshore oil activity is a greater probability of oil spills in the coastal zone. The transport, transformation, and fate of oil spilled in the sea remains the subject of ongoing study, with a comprehensive update compiled recently by the National Research Council (*2*). An important emerging issue is the fate of heavy oils introduced into the sea, where heavy oil is defined here as having API gravity of <17 . Heavier oil often has a substantially greater proportion of the high molecular weight resin and asphaltene fractions.

To address the fate of heavy oil in the coastal ocean, we turned to the natural seeps at Coal Oil Point (COP), offshore Goleta, CA. These seeps provide a unique setting to investigate the transport, transformation, and fate of heavy oil in the sea, as they provide a consistent input of oil to the coastal ocean and are readily accessible (*3*). Active oil seeping from this location can be viewed in the video accompanying this work. The oil emanating from the seeps is derived from the Monterey Formation and comprised of ∼30% hydrocarbons and ∼70% resins plus asphaltenes (*4, 5*). These seeps have been active for hundreds to thousands of years (*6, 7*) and have served as a study site for numerous previous investigations (recent works by Wardlaw et al. (*8*), Del Sontro et al. (*9*), and Mau et al. (*10*), and references therein).

Previous studies of COP seep oil have also addressed the subsurface biodegradation of oil (*8*), initial physical weathering of surface slicks (*8*), wind-driven evolution of surface slicks over short time scales (<2 h) (*11*), and tar accumulation and transport on local beaches (*9*). However, we are aware of no published studies in which the long-term fate of COP oil is quantified in sediments. Additionally, marine sediments are known to retain oil for longer than contaminated beaches or open ocean environments (*12*). Here, we assess the oil burden in an area west of the COP seep field to determine the magnitude of oil deposited from the COP seep field into the benthic environment. Furthermore, we assess the patterns and extent of hydrocarbon weathering in seep oils deposited to the sediments. Sediment grab samples were collected down current from the seep field, analyzed for hydrocarbon content using gas chromatography with flame ionization detection (GC-FID) and comprehensive two-dimensional gas chromatography with time-of-flight mass spectrometry (GC × GC-ToF-MS), and the resulting spatial variations were related to regional current patterns as determined with a high-frequency radar array and current meters.

Experimental

Sediment Sampling and Bulk Analyses. Sediment samples were collected at 15 locations in a 90 km^2 grid starting 4 km west of the COP seep field on July seventh, 2007 from the *R/V Atlantis*. Sample stations were arranged in five longitudinal transects with three water depths (40, 60, and 80 m) for each transect, with one additional comparison sample obtained from within the seep field (labeled BC-16). The locations of each sample are provided in Table S1 and Figure S1. The samples were collected using a small grab-core sampling device with a collection volume of 3000 cm^3 (10 cm × 12 cm × 25 cm). Subsamples were taken from the top 3−5 cm of sediment using a solvent-cleaned stainless steel spoon, sealed in glass jars with PTFE lined caps, and immediately placed in a −20 C freezer on board the *R/V Atlantis*. Samples were returned to the shore-based laboratory and analyzed for carbon and nitrogen abundance (CN), carbonate content, bulk organic carbon isotopic composition (δ^{13}C-TOC), and bulk nitrogen isotopic composition (δ^{15}N-TN), as described previously (*13, 14*). Bulk sediment density was measured for dried sediment (100 C for 24 h) with a Pycnometer (AccuPyc 1330).

* Corresponding author phone: 805-893-2973; fax: 805-893-2314; e-mail: valentine@geol.ucsb.edu.

[†] Department of Earth Science and Marine Science Institute, University of California, Santa Barbara.

[‡] Department of Marine Chemistry and Geochemistry, Woods Hole Oceanographic Institution.

[§] Department of Geography and Marine Science Institute, University of California, Santa Barbara.

10.1021/es802586g CCC: $40.75 © 2009 American Chemical Society
Published on Web 03/05/2009

Hydrocarbon Extraction and GC-FID Analysis. Air-dried sediment (1−6 g) was spiked with internal standards: 40 μg of perdeuterated heptadecane (nC$_{17}$-d_{34}; Cambridge Isotope Laboratories) and 1 μg of C$_{27}$ α(20R) cholestane-d_4 (Chiron). Each sample was extracted with a 9:1 dichloromethane (DCM)/methanol mixture by pressurized fluid extraction (100 C, 1000 psi). For total lipid extract (TLE) analysis, ∼12% of each sample was transferred to a tared 4 ml vial. The solvent was allowed to evaporate at room temperature in a laboratory hood and then the vial was reweighed. The material remaining in the vial was operationally defined as the TLE. All or some of the remaining extract was solvent exchanged into hexane, reduced to 1 mL via rotary evaporation, and charged onto a glass column (9 cm × 0.4 cm) packed with fully activated silica gel (100−200 mesh) over a small layer (1 cm) of activated copper granules (−10 + 40 mesh, 99.90+%). The column was eluted with 12 mL of a 3:1 mixture of hexane/DCM to elute saturated and aromatic hydrocarbons. Each extract was reduced to a small volume (100 μL), spiked with the external standard dioctyl ether (40 μg), and analyzed on a Hewlett-Packard 5890 Series II gas chromatograph with a flame ionization detector. A 1 μL sample was injected cool-on-column. Compounds were separated on a glass capillary column (J&W DB-1MS, 30m, 0.25 mm i.d., 0.25 μm film thickness) with H_2 as the carrier gas at a constant flow of 5 mL min^{-1}. The GC oven temperature was programmed from 45 (5 min hold) to 315 C at 6 min^{-1} and then from 315 to 320 C at 20 min^{-1} (30 min hold). Response factors were generated with calibration solutions of Supertech motor oil SAE 10W-30 relative to nC$_{17}$-d_{34}. Operationally defined GC-amendable total petroleum hydrocarbons (TPHs) were quantified by integrating the total detector signal for the unresolved complex mixture (UCM). The total area of the UCM relative to the nC$_{17}$-d_{34} along with the response factors were used to calculate TPH content. All sediment data is presented on a dry weight basis.

Laboratory blanks of combusted sand were free of petroleum compounds. The average percent recovery of the nC$_{17}$-d_{34} was 78 ± 5%. To gauge the overall effectiveness of the method, motor oil was spiked into combusted sand and analyzed − 100% recovery was observed. Precision, on the basis of replicate analysis of three samples, was 7 to 8% for TLE and 5 to 20% for TPH.

Each sample was also analyzed using GC × GC-ToF-MS according to the procedures of Wardlaw et al. (*8*). Detailed instrumental parameters can be found in the methods of the Supporting Information.

Reference Samples. Reference samples were taken from our collection and included reservoir oils from beneath the COP seep field (Platform Holly), reservoir oils from elsewhere in the Monterey formation (Platform Gail, located ∼15 km southeast of the seep field), and oil actively seeping from the sea floor at a location known as Jackpot seep − as described in Wardlaw et al. (*8*). Additional samples analyzed from our collection included oils from other formations and freshly seeped oils collected from the sea surface overlying several named seeps (Trilogy, Horseshoe, and La Goleta) within the COP seep field. See Del Sontro et al. (*9*) for locations of these named seeps. Oil samples were extracted into hexane and analyzed with GC × GC-ToF-MS as described in the methods of the Supporting Information. Oil collected from a fresh slick overlying Trilogy seep was also analyzed using GC-FID as described previously.

Results and Discussion

Study Site and Oil Source. Sediment sampling sites were chosen at three depths (40, 60, and 80 m) along each of five longitudinal transects located to the west of the COP seep area (Figure S1 and Table S1, encompassing ∼90 km^2 of the continental shelf and spanning the approximate depth range of the seeps. The results of bulk chemical analyses for all of the core samples are provided in Table S1 and clearly demonstrate that these samples are impacted by oil. To assess the source of this oil, GC × GC-ToF-MS was applied to determine the ratios of hopane biomarkers for each sample, enabling a comparison among these samples, fresh oil slicks from the COP seep field, reservoir oils underlying the seep field, and other reference oils. Results from this comparison are presented in Table S2 and Figure S2. Similarities in the distribution and relative abundance of hopane biomarkers between all sediment samples, reservoir material from the seep field, and seep oil strongly suggest that oils derived from the Monterey formation, such as those seeping from COP, serve as the primary source of petroleum to these sediments. These similarities are displayed as a graphic comparison of GC × GC-ToF-MS chromatograms for the biomarker region (Figure S2) for fresh oil collected from the sea surface at Trilogy seep and sediment sample BC-14. These similarities are further supported by the hopane abundance ratios presented in Table S2. A comparison of average values for four of these ratios is provided in Table 1 for sediment, seep, reservoir, and reference material and good agreement is observed between the measured values and previous work (*15*−*19*). To address whether Monterey oils other than those from COP might accumulate in the study area, a comprehensive search of the seep literature was conducted. No studies documenting active oil seepage in the study area were located, though known oil seeps exist to both the east (COP) and the west (*20*) of the study area, and gas seeps have been reported along the Molino anticline (*21*) located to the south. Satellite-based observations (*22*) further indicate that surface slicks in the study area originate from COP. More anecdotal observations from both aerial photos and routine trips throughout the study area suggest the transport of surface slicks from the COP seep field. On the basis of the available evidence, we contend that the COP seep field is the major source of oil deposition to the study area.

TABLE 1. Average Biomarker Ratios for Sediment, Seep, and Reservoir Samples

	Tm/Ts[a]	triplet[b]	H/NH[c]	H/BNH[d]
sediment (n = 16)	3.8 ± 0.2	4.2 ± 0.2	1.1 ± 0.1	0.76± 0.13
seep (n = 6)[e]	3.8 ± 0.3	4.1 ± 0.1	1.2 ± 0.1	0.72 ± 0.18
reservoir (n = 3)	3.8 ± 0.3	NR	1.1 ± 0.03	0.70 ± 0.04
Exxon Valdez (n = 1)	1.3	1.7	1.2	30.5

[a] Tm/Ts represents the ratio of 22,29,30-trinor-18α(H)-neohopane to 22,29,30-trinor-17α(H)-hopane. [b] Triplet represents the ratio of C$_{26}$ tricyclicterpanoids (S+R epimers) to C$_{24}$ tetracyclicterpanoid. [c] H/NH represents the ratio of 17α-(H),21β(H)-hopane to 17α(H),21β(H)-30-norhopane. [d] H/BNH represents the ratio of 17α(H),21β(H)-hopane to 17α-(H),21β(H)-28,30-bisnorhopane. [e] n = 5 for triplet, NR = not reported.

Fallout Plume. The concentration of TLE in sediments generally decreased with distance from the seep field (Table S1). Sediment collected within the seep field (sample BC-16) comprised of 3.2% TLE by mass, with the TLE accounting for 65% of the total organic carbon (TOC) present in the sediment. Sediments outside of the seep field had TLE levels ranging from 0.09 wt % away from the seeps to 0.73 wt % near to the seeps, with TLE accounting for 14 to 42% of TOC. The concentration of TPH follows an almost identical trend to that of TLE, as supported by the consistent TPH to TLE ratio (0.21 ± 0.03, n = 16) presented graphically in Figure S3.

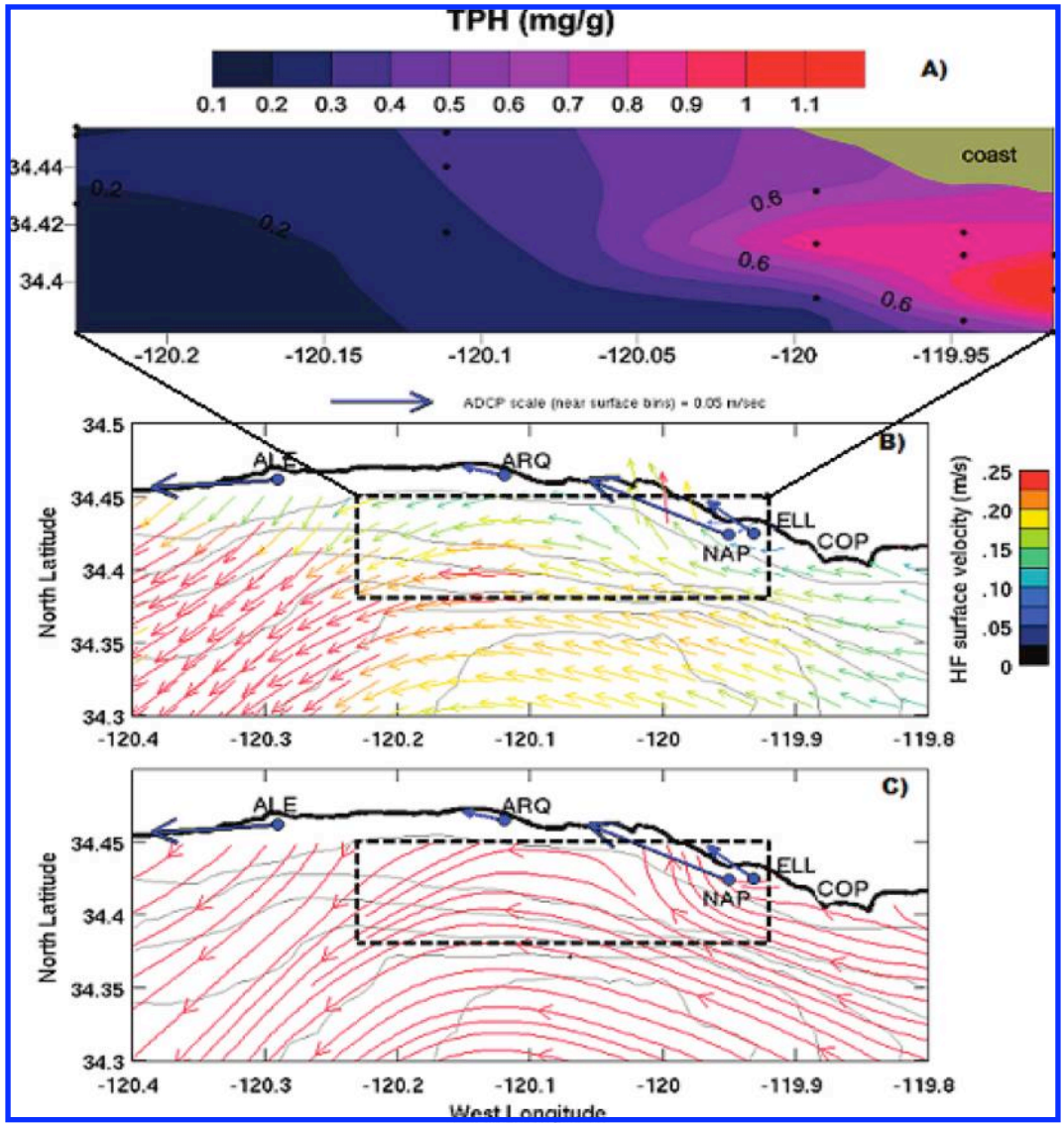

FIGURE 1. A) Fallout plume contour plot of TPH concentration for 15 selected sample sites (black dots) shown in conjunction with B) mean surface current (upper 1 m) vectors derived from HF radar for 2000−2007 in and around the study area and; C) particle paths computed from mean current vectors shown in B. Current speeds are color coded according to the scale bar to right of the center panel. Blue arrows near shore are current vectors in the upper water column (depth range approximately 2−4 m) from acoustic Doppler current meters deployed along the 15 m isobath at Ellwood (ELL), Naples Reef (NAP), Arroyo Quemado (ARQ), and Alegra (ALE). The speed scale for these vectors is indicated above the panel. Fine black lines are bathymetric contours at 50, 100, 200, 300, 400, and 500 m. The lower panel shows particle paths computed from the mean current vectors of the center panel. Arrow heads indicate flow direction. Upstream ends of lines are starting points of particle tracks along HF radar coverage boundary. Particle track beginning near 34.42 N, 120 W suggests bifurcation of mean flow trajectories: one branch flows shoreward west of COP, the other branch curves offshore.

The spatial distribution of sediment TPH displayed in contour form (Figure 1) reveals a trend of elevated TPH centered around 60 m water depth, with concentrations generally decreasing in both inshore and offshore directions. This distribution suggests a selective input of seep oil at or around this depth. To assess whether ocean surface currents control the distribution of TPH and TLE in sediments, current velocity data were collected from a high-frequency radar array (*23, 24*) and bottom mounted acoustic Doppler current profilers along the 15 m isobath. The current pattern averaged during 2000−2007 over the study area and the COP seep field shows a clear relationship to the distribution of sediment TPH (Figure 1). The patterns of sediment TPH abundance and surface currents suggest that most oil from the COP seeps is not transported large distances but rapidly weathers at the sea surface and then sinks to the sea floor. On the basis of mean current speeds of 0.07−0.15 m s^{-1} and flow path lengths from COP seeps to sampling locations of 5−30 km, sinking times range from about 0.4−5 days. An upper bound on the sinking rate is ∼200 m day^{-1}.

The results presented here strongly suggest that seeped oil from COP is incorporated into sediments nearby to the seep field, as controlled by the surface currents. Two basic mechanisms might account for this observation. One mechanism involves rapid weathering of the abundant surface slicks at COP by evaporative or biological processes. For Monterey-derived oils, such weathering increases oil density through selective removal of light hydrocarbons (*8*). The residual oil becomes enriched in high molecular weight fractions, likely until it exceeds ambient seawater density and sinks to the sea floor. Assuming this mechanism and using the sinking rate of 200 m day^{-1} inferred above, the implied ratio of oil density to seawater density is in the range 1.00005−1.005 using Stokes law (*25*) with oil particle diam-

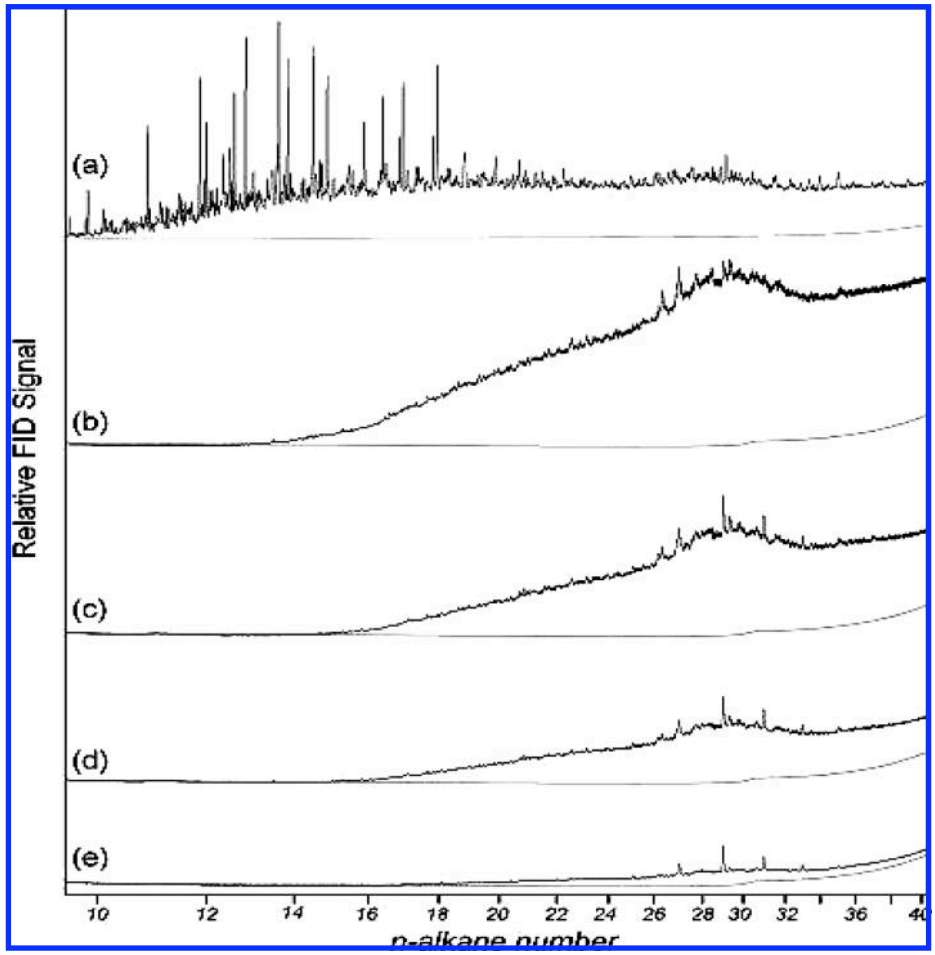

FIGURE 2. GC-FID chromatograms of (a) a fresh oil slick and (b−e) sediment samples collected progressively further from the COP seeps. a) slick oil collected from the sea surface above Trilogy seep; b) sea-floor sediment sample # BC - 16 collected from the seep field at 50 m water depth; c−e) sediment samples BC - 14, BC - 11, and BC - 02, respectively − all located at 60 m water depth. See Figure S1 of the Supporting Information for specific sample locations. The UCM in chromatograms b−e is observed to decrease indicating decreasing TPH content with distance from the seeps. The dashed line at the base of each chromatogram is the solvent blank.

eters of 1−10 cm. Considering the origin of the seep oil, the timing of this weathering process, and the average velocity of surface currents, it seems likely that the oil is weathered at the surface and simultaneously transported by the currents until it deposits in the characteristic pattern displayed in Figure 1. While consistent with the data presented here, this mechanism is not consistent with some previous work (*9*) that suggested that winds, not currents, control the movement of surface slicks at COP. However, the prevailing northwest winds over coastal waters near COP are often weak so under these conditions westward currents, such as shown in part B of Figure 1 and documented in other studies (*22, 26−29*), can transport the oil westward.

A second possible mechanism consistent with the TPH and current velocity distributions is the benthic transport of oil-laden sediment westward from the seep field. Oil is deposited in the seep field through both surface weathering/sinking and by the weathering of fresh seep oil at the seafloor. This mechanism is not limited to oil that remains on the sea floor following emission. The action of winds as mentioned above leads to the stranding of oil from surface slicks on beaches around the COP seep field (*9*). Such stranding provides an alternative pathway to increased density of surface slick oil by sand incorporation (*30*). Sediment-impacted oil of higher density would then be returned to the coastal ocean through tides and wave action. Previous studies have shown that subsurface currents along the mainland coast and deeper in the Santa Barbara Channel have similar directions as surface currents (*28, 31*).

Thus, it is likely that oily sediments resuspended in the bottom waters are transported to the west and settle in a pattern consistent with that observed. A combination of the two mechanisms is also possible. We suggest the terms "fallout plume" or "tar shadow" to describe the deposition that may result from either or both mechanisms.

The consistency between the spatial distribution of TPH in sediment and the annual surface currents (Figure 1), along with other lines of evidence discussed above, strongly suggest that oil in the study region originates from the COP seep field. This is further supported by the observed gradient in sediment oil content, which decreases with distance from the COP field, and by the observation of low oil concentrations at the easternmost stations, which are situated closest to the oil seep located ~21 km to the west (*20*).

Oil Weathering. The consistency observed in the TPH to TLE ratio among sediment samples suggests that hydrocarbon weathering approaches a common, finite limit. The GC-FID traces in Figure 2 are consistent with this observation as they show the same distribution of TPH within the UCM in four sediment samples, indicating dilution of oil content rather than increased weathering distal from the seep field.

As summarized in Figure 2, sediment samples all displayed a pronounced UCM when compared to fresh slick oil, demonstrating a high degree of weathering. The lone

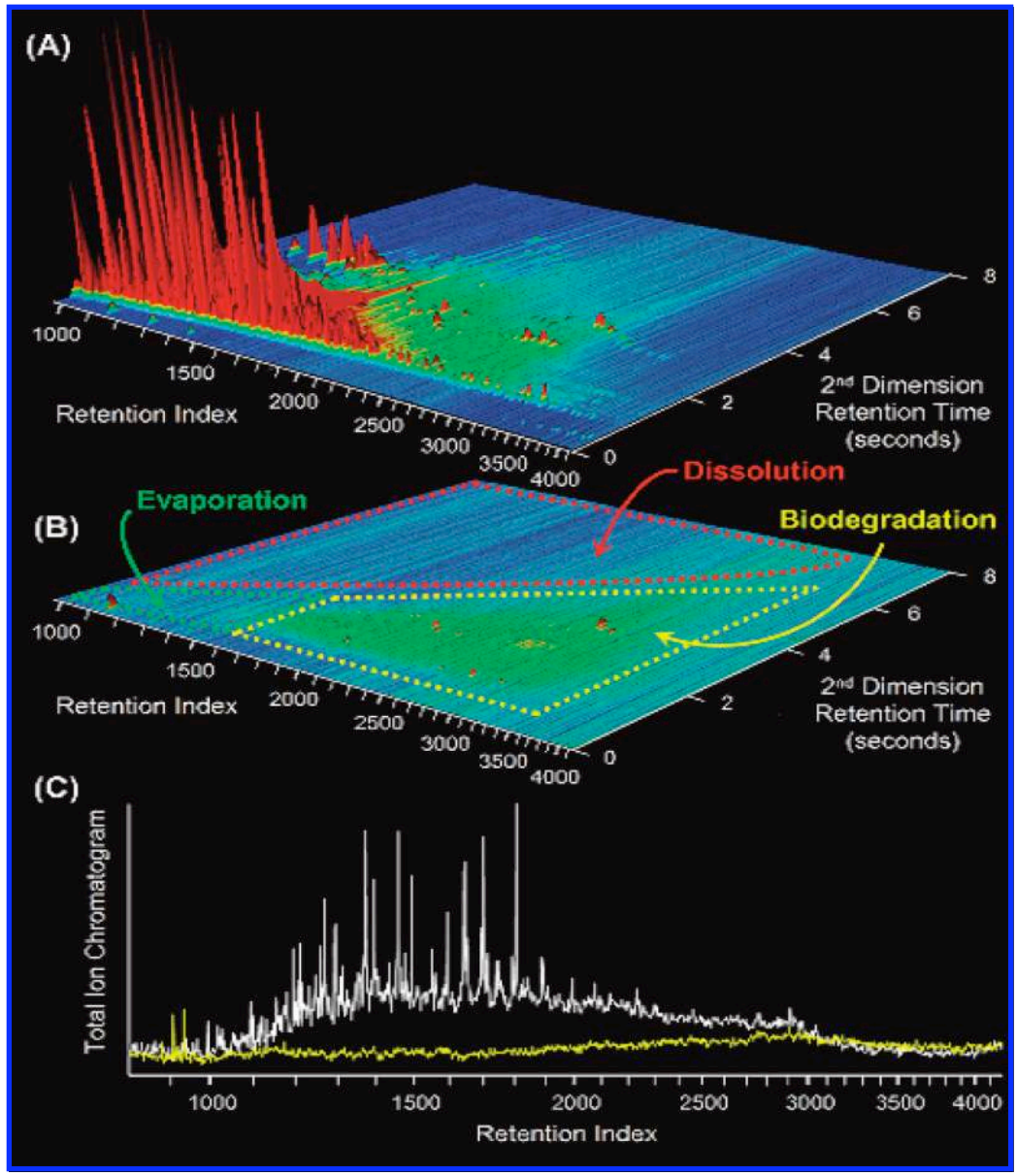

FIGURE 3. GC × GC-ToF-MS chromatograms of A) surface slick oil collected from the sea surface above Trilogy seep; B) sediment sample oil from BC - 14, with regions of the chromatogram marked corresponding to the likely associated forms of weathering; and C) comparison of TIC traces from panels A (white) and B (yellow) collapsed into one dimension. Retention indices in all three panels are consistent with carbon number, i.e. RI = 1000 is *n*-C_{10}, RI = 1500 is *n*-C_{15}, etc., and each chromatogram is scaled to 17α(H),21*β*(H)-28,30-bisnorhopane.

sediment sample taken from within the seep field also displayed a large UCM (part b of Figure 2), though notably the ratio of TPH to TLE was greater for this sample than any other (Table S1 of the Supporting Information). To better assess the molecular patterns associated with weathering, we compared GC × GC-ToF-MS chromatograms from select samples in total ion current (TIC) mode. Results typical of this comparison are presented graphically in Figure 3 for a fresh seep oil and sediment sample oil and clearly display the loss of numerous hydrocarbons. Compound classes lost to weathering include *n*-alkanes, isoprenoidal alkanes, alkylcyclopentanes, alkylcyclohexanes, alkylbenzenes, and many alkylated PAHs − leaving sediment oil dominated by recalcitrant biomarkers such as hopanes and diasteranes.

We suggest that the observed loss pattern (Figure 3) results from a combination of evaporation, dissolution, and biodegradation, with only a minor contribution from photooxidation or other processes. Evaporation and dissolution act on compounds eluting early on the *x* axis and late on the *y* axis respectively, as described by Arey et al. (*32, 33*). Evaporation would likely be limited to the time oil resides at the sea surface, as opposed to dissolution, which would occur both in the slick and after deposition into the sediment. For COP seep oil, a significant portion of TPH (∼10%) was observed to evaporate within minutes of an oil droplet reaching the sea surface (*8*).

However, on the basis of considerations of volatility, evaporation is unlikely to significantly impact compounds less volatile than ∼*n*-C_{16}, in good agreement with the results presented in Figures 2 and 3 and the time scale for transport and deposition. Wardlaw et al. (*8*) noted no significant dissolution of hydrocarbons for freshly seeped COP oils, but the exposure time was much shorter than for these oils, and it seems likely that the more polar polycyclic aromatic hydrocarbons gradually dissolve into seawater during slick migration and after deposition.

Aerobic biodegradation of petroleum in the surface slick and sediments is presumed to remove hydrocarbons

remaining after evaporation and dissolution (e.g., part B of Figure 3) and may compete with these physical loss processes for some compounds. Wardlaw et al. (*8*) established the perspective of broad metabolic specificity in anaerobic hydrocarbon-degrading communities, reporting the metabolism of over 900 distinct compounds. We suspect that a greater generality in hydrocarbon degradation exists within aerobic microbial communities. On the basis of the loss pattern in Figure 3, numerous compounds can be linked to biodegradation. These apparently biodegraded compounds range in size from ~16−42 carbons and include *n*-alkanes, branched alkanes, isoprenoids, alkyl cyclopentanes, alkyl cyclohexanes, alkyl benzenes, and alkyl napthalenes among others. These compounds constitute a significant portion of the nonweathered material in part A of Figure 3 and implicate biological degradation as an important source of weathering in Figure 2 and part B of Figure 3. Residual hydrocarbons remaining after biodegradation are highly insoluble, nonvolatile, and generally demonstrate structural complexity such as multiple rings and numerous tertiary carbons − all factors that tend to hinder remineralization.

Like biodegradation, photooxidative processes are relevant to compounds resistant toward evaporation, and this process should be considered here on account of the potential light exposure of the oil slicks. Photooxidation preferentially degrades alkyl-substituted PAHs (*34*). Plata et al. (*35*) determined the photolytic half-lives of susceptible multiring PAHs benzo[*a*]pyrene and chrysene to be 40 ± 10 days and 35 ± 7 days respectively on beaches exposed to a spill of heavy oil. Applying the calculated annual current velocities to the approximately 3 km distance between the COP seeps and sample station BC-14, slick migration time to this station is on the order of ~6 h. The discrepancy between the photolytic half-life of susceptible PAHs and the calculated migration time suggests that photooxidation is likely not a significant cause of weathering in this sample set. Also, saturates such as *n*-alkanes, isoalkanes, and cycloalkanes are not susceptible to photooxidation, (*36*) supporting our contention that aerobic biodegradation is likely the primary removal process for nonpolar compounds larger than ~*n*-C_{16}.

Magnitude of the Fallout Plume. The extensive fallout plume west of COP results from chronic deposition of oil into shelf sediments off central California and provides a rare case study to track the fate of heavy oil released into the coastal ocean. The mass of oil in this plume can be estimated with the data presented here (see the Supporting Information for a description of this calculation). By considering the spatial extent of the plume (90 km^2), we estimate it contains approximately 3.1×10^{10} g of petroleum in the top 5 cm of sediment. By assuming a homogeneous depth distribution, and sediment isopach thickness of 0.5 to 5.0 m in this region, we estimate a total petroleum burden of 0.31−3.1 Tg, equivalent to 8−80 spills the size of the *Exxon Valdez* disaster. Assuming a minimum emission of 100 barrels d^{-1} (*3*) from the COP seep field with an average TPH/TLE of 0.49, this quantity of oil is equivalent to 0.45−4.5 Tg of fresh seep oil, or 80 to 800 years of seepage from the COP field. The clear control imparted by currents on the distribution of the oil is surprising, as is the proximity of deposition to the source, the common level of weathering observed in all sediments, and the overall amount of oil residing in the study area. These results may prove useful in combating future spills of heavy oils and underscore the utility of investigating natural marine oil seeps.

Acknowledgments

We thank George Wardlaw, Steve Horner, Christopher Stubbs, and Heather Coleman for their sampling assistance, as well as the captain and crew of the R/V Atlantis and the scientific party of the SEEPS 07 cruise for operational support. Funding for this work was provided by the NSF (OCE-0447395 CAREER award to D.L.V.) and by the DOE (DE-FG02-06ER15775 to C.M.R.). Additional funding was provided through the Research Internships in Science and Engineering program at UCSB as well as through the Undergraduate Research and Creative Activities program at UCSB (to C.F.).

Supporting Information Available

Detailed description of the analytical methods employed in this study and a comprehensive list of biomarker parameters and properties identified for the sample set. This material is available free of charge via the Internet at http://pubs.acs.org.

Literature Cited

(1) Edwards, J. D. Crude oil and alternate energy production forecasts for the twenty-first century; the end of the hydrocarbon era. *AAPG Bulletin* **1997**, *81* (8), 1292–1305.
(2) National Research Council, *Oil in the Sea III: Inputs, Fates, and Effects.* National Academies Press: Washington, D.C., 2003; p 265.
(3) Hornafius, J. S.; Quigley, D.; Luyendyk, B. P., The world's most spectacular marine hydrocarbon seeps (Coal Oil Point, Santa Barbara Channel, California): Quantification of emissions. *J. Geophys. Res.-Oceans* 1999, *104*, (C9), 20703−20711.
(4) Reed, W. E.; Kaplan, I. R. Chemistry of marine petroleum seeps. *J. Geochem. Explor.* **1977**, *7* (2), 255–293.
(5) Stuermer, D. H.; Spies, R. B.; Davis, P. H.; Ng, D. J.; Morris, C. J.; Neal, S. The hydrocarbons in the Isla Vista marine seep environment. *Mar. Chem.* **1982**, *11* (5), 413–426.
(6) Hill, T. M.; Kennett, J. P.; Valentine, D. L.; Yang, Z.; Reddy, C. M.; Nelson, R. K.; Behl, R. J.; Robert, C.; Beaufort, L. Climatically driven emissions of hydrocarbons from marine sediments during deglaciation. *Proc. Natl. Acad. Sci. U.S.A.* **2006**, *103* (37), 13570–13574.
(7) Boles, J. R.; Eichhubl, P.; Garven, G.; Chen, J. Evolution of a hydrocarbon migration pathway along basin-bounding faults: Evidence from fault cement. *AAPG Bulletin* **2004**, *88* (7), 947–970.
(8) Wardlaw, G. D.; Arey, J. S.; Reddy, C. M.; Nelson, R. K.; Ventura, G. T.; Valentine, D. L. Disentangling oil weathering at a marine seep using GC×GC: Broad metabolic specificity accompanies subsurface petroleum degradation. *Environ. Sci. Technol.* **2008**, *42* (19), 7166–7173.
(9) Del Sontro, T. S.; Leifer, I.; Luyendyk, B. P.; Broitman, B. R. Beach tar accumulation, transport mechanisms, and sources of variability at Coal Oil Point, California. *Mar. Pollut. Bull.* **2007**, *54* (9), 1461–1471.
(10) Mau, S.; Valentine, D. L.; Clark, J. F.; Reed, J.; Camilli, R.; Washburn, L. Dissolved methane distributions and air-sea flux in the plume of a massive seep field, Coal Oil Point, California. *Geophys. Res. Lett.* **2007**, *34*, (22).
(11) Leifer, I.; Luyendyk, B.; Broderick, K. Tracking an oil slick from multiple natural sources, Coal Oil Point, California. *Marine and Petroleum Geology* **2006**, *23* (5), 621–630.
(12) Boehm, P. D.; Steinhauer, M. S.; Green, D. R. Comparative fate of chemically dispersed and beached crude oil in subtidal sediments of the arctic nearshore. *Arctic* **1987**, *40*, 133–148.
(13) Ding, H.; Valentine, D. L. Methanotrophic bacteria occupy benthic microbial mats in shallow marine hydrocarbon seeps, Coal Oil Point, California. *J. Geophys. Res.-Biogeosciences* **2008**, *113*, (G1).
(14) Valentine, D. L.; Kastner, M.; Wardlaw, G. D.; Wang, X. C.; Purdy, A.; Bartlett, D. H., Biogeochemical investigations of marine methane seeps, Hydrate Ridge, Oregon. *J. Geophys. Res.-Biogeosciences* **2005**, *110*, (G2).
(15) Crisp, P. T.; Brenner, S.; Venkatesan, M. I.; Ruth, E.; Kaplan, I. R. Organic-chemical characterization of sediment-trap particulates from San Nicolas, Santa Barbara, Santa Monica and San Pedro basins, California. *Geochim. Cosmochim. Acta* **1979**, *43* (11), 1791–1801.
(16) Hostettler, F. D.; Rosenbauer, R. J.; Lorenson, T. D.; Dougherty, J. Geochemical characterization of tarballs on beaches along the California coast. Part I - Shallow seepage impacting the Santa Barbara Channel Islands, Santa Cruz, Santa Rosa and San Miguel. *Org. Geochem.* **2004**, *35* (6), 725–746.

(17) Isaacs, C. M.; Rullkotter, J., *The Monterey Formation: From Rocks to Molecules*, 1st ed.; Columbia University Press: New York, 2000, p 608.
(18) Kvenvolden, K. A.; Hostettler, F. D.; Carlson, P. R.; Rapp, J. B.; Threlkeld, C. N.; Warden, A. Ubiquitous tar balls with a California-source signature on the shorelines of Prince William Sound, Alaska. *Environ. Sci. Technol.* **1995**, *29* (10), 2684–2694.
(19) Mangelsdorf, K.; Rullkotter, J. Natural supply of oil-derived hydrocarbons into marine sediments along the California continental margin during the late Quaternary. *Org. Geochem.* **2003**, *34* (8), 1145–1159.
(20) Vernon, J. W.; Slater, R. A. Submarine tar mounds, Santa Barbara county, California. *AAPG Bulletin* **1963**, *47* (8), 1624–1627.
(21) Eichhubl, P.; Greene, H. G.; Naehr, T.; Maher, N. Structural control of fluid flow: offshore fluid seepage in the Santa Barbara Basin, California. *J. Geochem. Explor.* **2000**, *69−70*, 545–549.
(22) DiGiacomo, P. M.; Washburn, L.; Holt, B.; Jones, B. Coastal pollution hazards in Southern California observed by SAR imagery: Stormwater plumes, wastewater plumes, and natural hydrocarbon seeps. *Mar. Pollut. Bull.* **2004**, *49*, 1013–1024.
(23) Ohlmann, C.; White, P.; Washburn, L.; Terrill, E.; Emery, B.; Otero, M. Interpretation of coastal HF radar-derived surface currents with high-resolution drifter data. *Journal of Atmospheric and Oceanic Technology* **2007**, *24* (4), 666–680.
(24) Emery, B. M.; Washburn, L.; Harlan, J. A. Evaluating radial current measurements from CODAR high-frequency radars with moored current meters. *Journal of Atmospheric and Oceanic Technology* **2004**, *21* (8), 1259–1271.
(25) Batchelor, G. K. *An Introduction to Fluid Dynamics*. Cambridge University Press: Cambridge, 1967.
(26) Bassin, C. J.; Washburn, L.; Brzezinski, M.; McPhee-Shaw, E. Sub-mesoscale coastal eddies observed by high frequency radar: A new mechanism for delivering nutrients to kelp forests in the Southern California Bight. *Geophys. Res. Lett.* **2005**, *32*, (12).
(27) Dever, E. P. Objective maps of near-surface flow states near Point Conception, California. *Journal of Physical Oceanography* **2004**, *34* (2), 444–461.
(28) Harms, S.; Winant, C. D. Characteristic patterns of the circulation in the Santa Barbara Channel. *J. Geophys. Res.* **1998**, *103* (C2), 3041–3065.
(29) Winant, C. D.; Dever, E. P.; Henderschott, M. C. Characteristic patterns of shelf circulation at the boundary between central and southern California. *J. Geophys. Res.* **2003**, *108*, (C2).
(30) Michel, J. *Assessment and Recovery of Submerged Oil: Current State Analysis*; United States Coast Guard Research and Development Center: Groton, CT, June 9, 2006; pp 1−36.
(31) Nishimoto, M. M.; Washburn, L. Patterns of coastal eddy circulation and abundance of pelagic juvenile fish in the Santa Barbara Channel, California, USA. *Mar. Ecol.: Prog. Ser.* **2002**, *241*, 183–199.
(32) Arey, J. S.; Nelson, R. K.; Reddy, C. M. Disentangling oil weathering using GC×GC. 1. Chromatogram analysis. *Environ. Sci. Technol.* **2007**, *41* (16), 5738–5746.
(33) Arey, J. S.; Nelson, R. K.; Plata, D. L.; Reddy, C. M. Disentangling oil weathering using GC×GC. 2. Mass transfer calculations. *Environ. Sci. Technol.* **2007**, *41* (16), 5747–5755.
(34) Garrett, R. M.; Pickering, I. J.; Haith, C. E.; Prince, R. C. Photooxidation of crude oils. *Environ. Sci. Technol.* **1998**, *32* (23), 3719–3723.
(35) Plata, D. L.; Sharpless, C. M.; Reddy, C. M. Photochemical degradation of polycyclic aromatic hydrocarbons in oil films. *Environ. Sci. Technol.* **2008**, *42* (7), 2432–2438.
(36) Prince, R. C.; Garrett, R. M.; Bare, R. E.; Grossman, M. J.; Townsend, T.; Suflita, J. M.; Lee, K.; Owens, E. H.; Sergy, G. A.; Braddock, J. F.; Lindstrom, J. E.; Lessard, R. R. The roles of photooxidation and biodegradation in long-term weathering of crude and heavy fuel oils. *Spill Science & Technology Bulletin* **2003**, *8* (2), 145–156.

ES802586G